

Trajectory Planning of Biped Robot for Running Motion

Tomoyuki Suzuki, Toshiaki Tsuji, *student member, IEEE*, and Kouhei Ohnishi, *Fellow, IEEE*

Department of System Design Engineering, Keio University, Yokohama, Japan

tomoyuki@sum.sd.keio.ac.jp tsuji@sum.sd.keio.ac.jp ohnishi@sd.keio.ac.jp

Abstract— In recent years, studies of biped locomotion have been developed rapidly. Biped robots are able to walk smoothly. In addition, there came some robots which were able to run. Walking and running will be basic performances of biped robots in future.

In this paper, we propose a new trajectory planning method, applicable to plan both walking and running motions. The two kinds of motions are treated as a unified trajectory. The trajectory consists of two phases; sinusoidal trajectory and parabolic trajectory. With this method, we plan walking and running motions for a biped robot in a unified manner, and switch between walking state and running state by parameter modification. We simulated and experimented with the proposed trajectory planning method.

I. INTRODUCTION

A. Background

In past, robots were only products of fantasy. They, however, have been real products recently and became great work forces substitute for human resources. Most industrial robots in operation today work in structured factories such as automated plants. Their ability is enhanced to operate more accurately and more rapidly in a closed environment.

In recent times, however, new kinds of robots for an open environment were needed; for example, demining robot, rescue robot, caring robot, and pet robot. “AIBO” was released by SONY Corporation in 1999 as the first pet robot. As above, robots are developed for a variety of applications now.

Among them, the rescue and caring robots need an ability to move over various places; mass of rubble, stairs, and the other spaces where people move over. Conventional wheeled robots are not able to do this sort of works.

There are several types of transfer mechanisms to act in unstructured spaces; crawler, biped, polyped, and so on. Above all, legged robots have an advantage to choose discrete landing points. A biped robot, particularly, is suitable for human environment since its structure is like a human body.

Walking motion of biped robots has been studied by many researchers energetically. “ASIMO” [1] by Honda Motor Co., Ltd., “HRP-2” [2] by National Institute of Advanced Industrial Science and Technology (AIST), and “QRIO” by SONY Corp. became hot topics in the mass media. All of them achieved human-like motions with the high-performance hardware and software.

The theory and the technology of “walking” by robots with two legs were established by the researches on these

robots. Biped robots which are able to walk are made as not only test models for development but also practical machineries.

And now, not only “walking” but also “running” by robots with two legs attract attention. If running was achieved, biped robots would be one of the useful transfer mechanisms, since the mobility of a biped robot is close to that of human.

Researches about running motion of biped robots have been advanced diligently and several robots achieved running; QRIO, HRP-2 Leg Module for Running [3], and ASIMO run in 3D space.

Abilities of biped robots have improved more and more. Thus, we predict that, in future, both walking and running will be basic performances of biped robots.

B. Related Works

There have long been many researches about bipedal locomotion [4][5][6]. One of the famous theories is the linear inverted pendulum mode (LIPM) [7][8] proposed by Kajita *et al.*. In LIPM, a biped robot is modeled as an inverted pendulum. The motion of the mass point of the pendulum is kept on a straight line in sagittal plane. With that, it is possible to plan the COG-trajectory of the robot with linear differential equations. It gives us a simple model and makes control of robots easily. ASIMO walks stably by the method of ZMP control. ZMP is the indicator of stability of walking motion [1].

On the other hand, about running, researchers studied mainly about hopping or jumping as the basis of running. Raibert established the basis of study of hopping robot [9]. He made robot models simple with hydraulic actuators. He also proposed control methods for the planar one-legged machine. The control system treats hopping, forward speed, and body attitude as three separated control problems. Many researchers studied on hopping robots with various structures [10].

Researchers came to use hopping or running robots with rotary actuators [11] in late years. Their structures were like human body. Most of the actuators, however, couldn't output enough torque for robots to jump up. Therefore, many researches were demonstrated only in simulations. The group of AIST, for example, studied about running motion with the model of the humanoid robot, “HRP-1”. They simulated and calculated necessary torque of each joint [12].

Biped robots in future will need abilities to walk and to

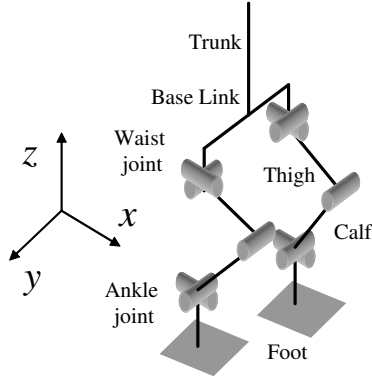
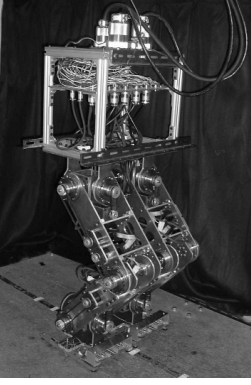


Fig. 1. Overview of biped robot

Fig. 2. 3D-model

run as basic performances. Trajectory for walking and that for running were planned separately in most researches. Hence, it will be useful that there is a trajectory planning method which treats both walking and running motions in a unified manner. In this paper, we proposed such a theory. We planned walking and running motions with a unified trajectory. It makes trajectory planning easy and with this method, switching between walking and running state became simple.

C. Overview of the Proposed Method

We propose a new trajectory planning method. One of its characteristics is to plan both walking and running motions in unified manner. It consists of two phases; sinusoidal trajectory and parabolic trajectory. With this method, trajectories are planned simply. In addition, it is possible to switch the state of biped robots between walking and running by parameter modification.

This paper is organized as follows. In section 2, we described the model of the biped robot, “Tomas-k”, and the kinematics. The control system to track planned trajectories is in section 3. In section 4, proposed trajectory planning method is explained. We demonstrated walking and running motion with our method in simulation in section 5. In section 6, we experimented in walking motion with the biped robot. Finally, we concluded the paper in section 7.

II. MODELING

A. Modeling

The robot we used is shown in Fig. 1. Fig. 2 shows the 3D-model of the robot. It is modeled as a mass system that each link has its weight on its COG. The robot has 10 DOF; 4 in frontal plane and 6 in sagittal plane.

Table I shows the parameters of each link of the robot.

B. Kinematics

The motion of each link was divided into translation component and rotational component. The motion of a robot was described with homogeneous transformation. Homogeneous transform matrix is represented as (1). It is expressed in base coordinate system, Σ_b . The origin of

TABLE I
THE PARAMETERS OF EACH LINK

	mass [kg]	length [m]	COG from upper joint [m]
Trunk	10.2	0.40	0.200
Waist joint link	2.6	0.00	-0.200
Thigh	3.5	0.30	0.126
Calf	3.4	0.30	0.095
Ankle joint link	2.6	0.00	-0.020
Foot	2.0	0.12	0.023

Σ_b is taken on base link position in Fig. 2.

$$\begin{bmatrix} \mathbf{P}_n \\ 1 \end{bmatrix} = \begin{bmatrix} {}^n\mathbf{R}_m & {}^n\mathbf{P}_m \\ 0 & 1 \end{bmatrix} \begin{bmatrix} \mathbf{P}_m \\ 1 \end{bmatrix} = {}^n\mathbf{T}_m \begin{bmatrix} \mathbf{P}_m \\ 1 \end{bmatrix} \quad (1)$$

\mathbf{P}_n : position in coordinate system based on joint n , Σ_n .
 \mathbf{P}_m : position in Σ_m . ${}^n\mathbf{P}_m$: position of joint m in Σ_n .
 ${}^n\mathbf{R}_m$: rotation matrix that converts position vector from in Σ_m to in Σ_n .

It is assumed that the soles of the robot didn't slip and direct kinematics are calculated with homogeneous transformation in global coordinate, Σ_g . The origin of Σ_g is on the ground.

$$\begin{bmatrix} \mathbf{x} \\ 1 \end{bmatrix} = \begin{bmatrix} \mathbf{R}_b & \mathbf{x}_0 \\ 0 & 1 \end{bmatrix} \begin{bmatrix} \mathbf{P}_b \\ 1 \end{bmatrix} \quad (2)$$

\mathbf{x} : position on the robot in Σ_g . \mathbf{x}_0 : position of the base link in Σ_g . \mathbf{P}_b : position vector in Σ_b . \mathbf{R}_b : rotation matrix from in Σ_b to in Σ_g .

On the other hand, to calculate inverse kinematics, we use a Jacobian matrix. The biped robot has 10-DOF. We controlled COG position with 3-DOF, the base posture with 2-DOF, the tip position of a swing leg with 3-DOF and that posture with 2-DOF. In this research, we plan trajectories in 2D and control the robot in 3D. An inverted pendulum model is used for trajectory planning and 10-link model is used for control. Joint angular acceleration reference values are calculated with (3) and (4).

$$\ddot{\boldsymbol{\theta}}^{ref} = \mathbf{J}_{cog}^+ \ddot{\mathbf{x}}_g^{ref} + (\mathbf{I} - \mathbf{J}_{cog}^+ \mathbf{J}_{cog}) \tilde{\mathbf{J}}_t^+ (\ddot{\mathbf{x}}_t^{ref} - \mathbf{J}_t \mathbf{J}_{cog}^+ \ddot{\mathbf{x}}_g^{ref}) \quad (3)$$

$$\tilde{\mathbf{J}}_t = \mathbf{J}_t (\mathbf{I} - \mathbf{J}_{cog}^+ \mathbf{J}_{cog}) \quad (4)$$

$\boldsymbol{\theta}$: joint angle vector. \mathbf{J}_{cog} : Jacobian matrix between the base link and COG. \mathbf{J}_t : Jacobian matrix between the base link and the tip of a swing leg. Superscript *ref* means the vector is a reference value and + means the matrix is an approximate inverse matrix. Subscript *cog* denotes the vector for COG, and *t* denotes the vector for the tip of the swing leg.

In this research, we consider the movement of the robot in sagittal plane.

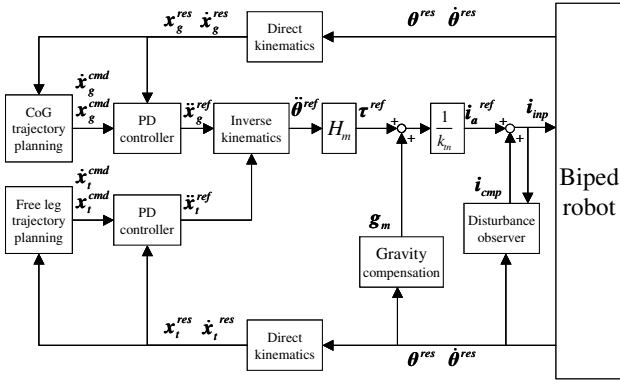


Fig. 3. Block diagram of entire control system

III. CONTROL SYSTEM

The main subject of this paper is a trajectory planning method. To track planned trajectories, we built up a control system with PD-controller and disturbance observer[13]. Disturbance observer was applied to the control system to compensate model error. Acceleration reference values as input are calculated in (5) and (6).

$$\ddot{x}_{cog}^{ref} = K_p (x_{cog}^{cmd} - x_{cog}^{res}) + K_v (\dot{x}_{cog}^{cmd} - \dot{x}_{cog}^{res}) \quad (5)$$

$$\ddot{x}_t^{ref} = K_p (x_t^{cmd} - x_t^{res}) + K_v (\dot{x}_t^{cmd} - \dot{x}_t^{res}) \quad (6)$$

K_p, K_v : feedback gain of PD-controller. Superscripts *res* means the vector is response value and *cmd* means the vector is command value.

Fig. 3 shows the entire control system.

IV. TRAJECTORY PLANNING

In this section, we explain the new COG trajectory planning method. Historically, trajectories for walking and for running were planned individually. With our method, they are unified and the new kind of trajectories is applied to both walking and running. It consists of two phases; sinusoidal trajectory and parabolic trajectory. With this, it is possible plan motions of walking and of running in a unified manner. Fig. 4 shows image of the trajectory in sagittal plane.

The two phases are based on running motion. In running motion, sinusoidal trajectory is a period that the robot touches the ground. On the other hand, parabolic trajectory is a period that the robot is in the air. Parabolic trajectory is also applied to walking motion. With that, walking and running motions are treated as a unified trajectory. Sinusoidal trajectory is planned to connect parabolic trajectory smoothly.

A. Threshold Value and Setting Parameters

In sinusoidal trajectory, the reaction force against the ground, F_z , is calculated in (7).

$$F_z = M(g - A\omega^2 \sin(\omega t)) \quad , \quad \omega = \sqrt{\frac{K_z}{M}} \quad (7)$$

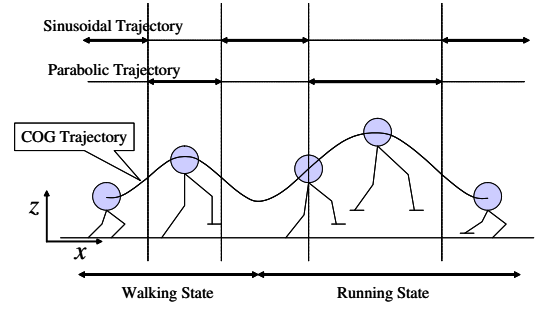


Fig. 4. COG-trajectory and robot motion

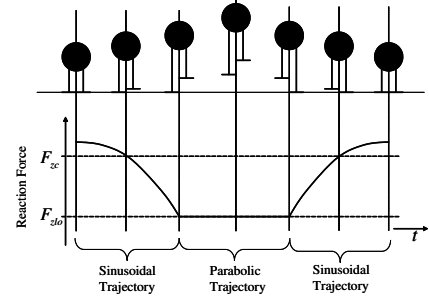


Fig. 5. Threshold and robot states

M : total mass of the robot. g : the gravity force. A : amplitude of the trajectory. ω : the natural resonance frequency. K_z : a virtual spring constant.

When $A\omega^2 > g$, F_z becomes less than zero and a robot jumps up. Threshold value F_{zlo} is defined for F_z , which is the boundary value between sinusoidal trajectory and parabolic trajectory. F_{zlo} takes value which meets (8) and (9).

$$M(g - A\omega^2) < F_{zlo} < M(g + A\omega^2) \quad (8)$$

$$0 \leq F_{zlo} \quad (9)$$

A and ω are given arbitrarily. Robot state is classified by F_{zlo} as Fig. 5.

A robot walks if $F_{zlo} > 0$, and runs if $F_{zlo} = 0$. Setting amplitude A and virtual spring constant K_z and choosing F_{zlo} , it is switched between walking state and running state. F_{zlo} is set at will.

B. Sinusoidal Trajectory ($F_z \geq F_{zlo}$)

In Sinusoidal trajectory, COG-trajectory in z direction is denoted as (10)~(12). They are expressed in Σ_g .

$$z(t) = z_0 + A \sin(\omega t + \delta) \quad (10)$$

$$\dot{z}(t) = A\omega \cos(\omega t + \delta) \quad (11)$$

$$\delta = \arcsin\left(\frac{g - \frac{F_{zlo}}{M}}{A\omega^2}\right) \quad (12)$$

z_0 : balanced height of COG. δ : phase difference between COG height at landing and z_0 . The initial and the end states are shown in (13) and (14).

$$z_{td} = z_{lo} = -(z_0 + A \sin(\delta)) \quad (13)$$

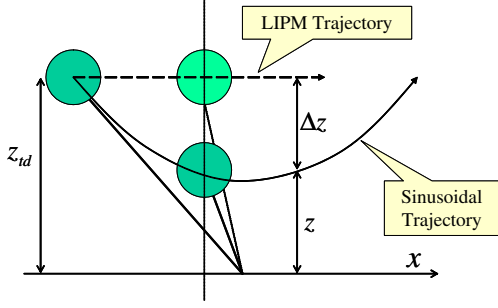


Fig. 6. Sinusoidal trajectory in sagittal plane

$$\dot{z}_{td} = -\dot{z}_{lo} = -\sqrt{(A\omega)^2 - \left(\frac{g - \frac{F_{zlo}}{M}}{\omega}\right)^2} \quad (14)$$

Subscript lo denotes the moment of lifting off and td denotes the moment of touching down. COG-trajectory in x direction is made based on LIPM, (15) and (16).

$$x_{linear} = x_0 \cosh \frac{t}{T_c} + T_c \dot{x}_0 \sinh \frac{t}{T_c} \quad (15)$$

$$\dot{x}_{linear} = \frac{x_0}{T_c} \sinh \frac{t}{T_c} + \dot{x}_0 \cosh \frac{t}{T_c} \quad (16)$$

$x_{linear}, \dot{x}_{linear}$: position and velocity in LIPM. x_0, \dot{x}_0 : initial position and velocity of the robot at $t = 0$. $T_c = \sqrt{\frac{z_c}{g}}$. z_c : z-intercept of trajectory line.

It is defined Δz as interval between COG-height of the sinusoidal trajectory and that of LIPM. COG-height of LIPM is set at constant value z_{td} (Fig. 6). The COG-trajectory in x direction is calculated by (17) and (18) that new terms proportional to Δz are added, to (15) and (16).

$$x = x_0 \cosh \frac{t}{T_c} + T_c \dot{x}_0 \sinh \frac{t}{T_c} + \int \frac{\Delta z}{l} \dot{x}_{linear} dt \quad (17)$$

$$\dot{x} = \frac{x_0}{T_c} \sinh \frac{t}{T_c} + \dot{x}_0 \cosh \frac{t}{T_c} + \frac{\Delta z}{l} \dot{x}_{linear} \quad (18)$$

C. Parabolic Trajectory ($F_z < F_{zlo}$)

In parabolic trajectory, the robot walks keeping the reaction force against the ground, F_z , constant value F_{zlo} . COG-trajectory in z direction is expressed in (19) in Σ_g .

$$z(t) = -\frac{1}{2} \left(g - \frac{F_{zlo}}{M} \right) t^2 + \dot{z}_{lo} t + z_{lo} \quad (19)$$

This section is classified into the case $A\omega^2 < g$ and the case $A\omega^2 \geq g$.

C.1 Parabolic Trajectory in Walking ($A\omega^2 < g$)

In this case, $F_z > 0$ and so the robot doesn't jump up. The sole of a support foot still contacts the ground and the robot is controlled to keep $F_z = F_{zlo}$. Tip commands of the support foot are shown in (20) and (21) in Σ_b .

$$z^{cmd} = \frac{1}{2} \left(g - \frac{F_{zlo}}{M} \right) t^2 + \dot{z}_{lo} t + z_{lo} \quad (20)$$

TABLE II
CONTROL PARAMETERS

Proportional Gain	K_p	2500.0
Derivative Gain	K_v	100.0
Sampling Time[s]	S_t	0.001
Observer Cutoff Frequency	g_{obs}	50.0
Threshold Value between Sinusoidal trajectory and Parabolic Trajectory [N]	F_{zlo}	$M(g - A\omega^2 * 0.7)$
Command Tip-position on Support-foot at Touch-down	x_0	0.05
Command Tip-velocity on Support-foot at Touch-down (walking) [m/s]	\dot{x}_0	0.915
Command Tip-velocity on Support-foot at Touch-down (running) [m/s]	\dot{x}_0	1.0

$$\dot{z}^{cmd} = \left(g - \frac{F_{zlo}}{M} \right) t + \dot{z}_{lo} \quad (21)$$

C.2 Parabolic Trajectory in Running ($A\omega^2 \geq g$)

In this case, if $F_{zlo} = 0$, the reaction force F_z becomes zero and a robot jumps up. COG trajectory is calculated in (22).

$$h = -\frac{1}{2} g t^2 + \dot{z}_{lo} t + z_{lo} \quad (22)$$

h : COG height in Σ_g . When the robot is in the air, both feet are above the ground. It is impossible to control COG Trajectory and the robot is controlled to prepare for the next landing. Tip commands of the feet are shown in (23)~(26) in Σ_b . T_1 : period of parabolic trajectory.

$$z_{cog}^{cmd} = z_{cog,lo} + (z_{t,td} - z_{cog,lo}) \frac{1 - \cos\left(\frac{t}{T_1}\right)}{2} \quad (23)$$

$$\dot{z}_{cog}^{cmd} = (z_{t,td} - z_{cog,lo}) \frac{1}{2T_1} \sin\left(\frac{t}{T_1}\right) \quad (24)$$

$$z_t^{cmd} = z_{t,lo} + (z_{cog,td} - z_{t,lo}) \frac{1 - \cos\left(\frac{t}{T_1}\right)}{2} \quad (25)$$

$$\dot{z}_t^{cmd} = (z_{cog,td} - z_{t,lo}) \frac{1}{2T_1} \sin\left(\frac{t}{T_1}\right) \quad (26)$$

We take $t = 0$ at the beginning of each phase. Position and velocity command are continuous at boundaries between the phases. COG-trajectory in x direction is planned to move forward with constant velocity.

V. SIMULATION

In this section, walking and running motions of a biped robot were simulated with the proposed trajectory planning method. The ground was modeled as a spring-damper model. For dynamics in simulation, we used the motion equation extended for a manipulator on mobile robot[14]. The robot has 6 DOF in sagittal plane and control parameters in Table II.

TABLE III
TRANSITION OF MAIN PARAMETERS

Steps	1	2~3	4~5	6~11	12~
Altitude A [m]	0.04	0.05	0.07	0.10	0.05
Virtual Spring Constant K_z	400	400	600	800	300

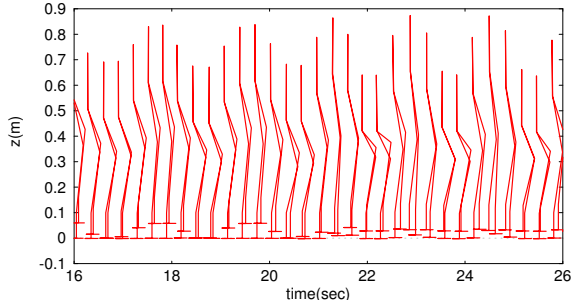


Fig. 7. Stick diagram

It is assumed that the gravity was 1.568m/s^2 (1/6 of the actual one) and the balanced height $z_0=0.5\text{m}$. Table III shows transition of the two main parameters. The transition from walking state to running state is schematically explained in Fig. 7. It shows the robot run and both feet were in the air.

The simulation results are shown in Fig. 8 ~ Fig. 10. Fig. 8 shows the relationship between time and the COG height from the ground, from the tip of the right foot, and from the tip of the left foot. When walking, the two length, COG height from the ground and that from the tip of the support foot, were the same. When running, the former is longer than the latter and it means that the robot was in the air.

These results demonstrated that it is easy to change states between walking and running with the proposed method.

There are, however, some difficulties and one of them is bounce at landing. We can find out this fact in Fig. 9. When $t \approx 21.0$, the reaction force on the ground was very large for a moment and it came to zero for a while. Suddenly, it jumped up to large value again when $t \approx 21.4$. The robot touched down twice at a landing. It is called "Hunting".

It was caused by difference between infall velocity of the robot and tip velocity of the support foot in z direction in Σ_g . To solve this problem, there are some approaches; building impedance control into the control system, and installing springs or buffer materials in the mechanics. The former has advantage to cushion impact and also has defect not to track planned trajectory properly. To overcome this difficulty is one of future works.

Fig. 10 is the graph with horizontal COG-position on the vertical axis and time on the lateral axis. It shows that the robot kept going ahead, switching between walking state and running state smoothly.

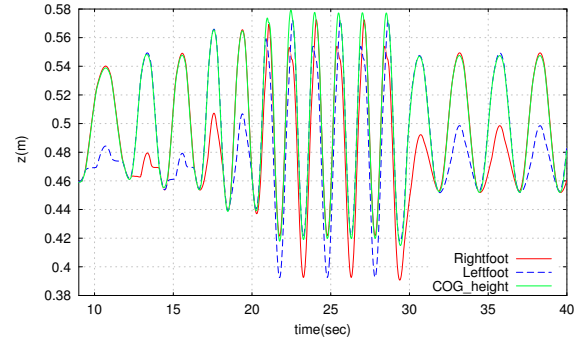


Fig. 8. Relationship between COG height and leg length in z direction

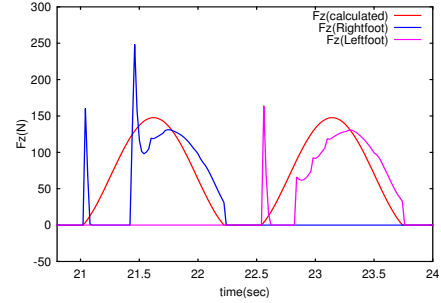


Fig. 9. Reaction force when running

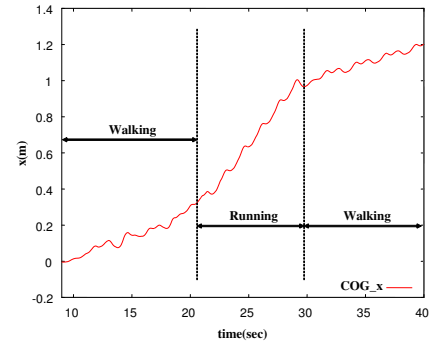


Fig. 10. COG trajectory in x axis in Σ_g

From these results, it was demonstrated that the proposed method makes trajectory planning of the biped robot simple, whichever walking or running.

VI. EXPERIMENT

In this experiment, we used the biped robot shown in Fig. 1. Table IV shows control parameters.

Balanced height $z_0=0.55\text{m}$, amplitude $A=0.04\text{m}$ and virtual spring constant $K_z=200\text{N/m}$. As the maximum torque of the motors was not enough for running motion, we only conducted experimentation of walking.

COG height from the ground changed in accord with the COG height from tip of the support foot as shown in Fig. 11. The robot kept walking without tipping over as shown Fig. 12. Fig. 13 shows ZMP data in x axis in Σ_g . While the robot walked, ZMP of the robot was always in stable area and it is shown that the robot walked stably. This experiment bore out effectiveness of the proposed method.

TABLE IV
CONTROL PARAMETERS

Proportional Gain	K_p	400
Derivative Gain	K_v	40
Sampling Time[s]	S_t	0.001
Observer Cutoff Frequency	g_{obs}	50
Threshold Value between Sinusoidal Trajectory and Parabolic Trajectory [N]	F_{zlo}	$M(g - A\omega^2 * 0.7)$
Command Tip-position on Support-foot at Touch-down [m]	x_0	0.05
Command Tip-position on Support-foot at Touch-down [m/s]	\dot{x}_0	0.875

VII. CONCLUSIONS

In this paper, we proposed a new trajectory planning method, which treats walking and running motions in a unified manner. The new trajectory consists of two phases; sinusoidal trajectory and parabolic trajectory. They are applicable to walking and running trajectory planning. With this method, it is possible to switch the walking state and running state simply by parameter modification.

We demonstrated the availability of the method by simulation and experiment. We simulated walking and running motions and the biped robot walked in experiment.

REFERENCES

- [1] K.Hirai, M.Hirose and T.Takenaka: "The Development of Honda Humanoid Robot," *Proceedings of the 1998 IEEE International Conference on Robotics & Automation*, pp. 1321-1326, 1998.
- [2] Shuuji Kajita, Fumio Kanehiro, Kenji Kaneko, Kiyoshi Fujiwara, Kensuke Harada, Kazuhito Yokoi and Hirohisa Hirukawa: "Biped Walking Pattern Generation by using Preview Control of Zero-Moment Point," *Proceedings of the 2003 IEEE International Conference on Robotics & Automation*, pp.1620-1626, September, 2003.
- [3] Shuuji Kajita, Takashi Nagasaki, Kenji Kaneko, Kazuhito Yokoi and Kazuo Tanie: "Running Control of Humanoid Biped HRP-2LR," *Proceedings of the 21st Annual Conference of the Robotics Society of Japan*, 2004.
- [4] Akihito Sano and Junji Furusho: "3D Dynamic Walking of Biped Robot by Controlling the Angular Momentum," *The Society of Instrument & Control Engineers*, Vol.26, No.4, pp. 459-466, 1990.
- [5] Kazuhisa Mitobe, Katsutomo Yajima and Yasuo Nasu: "Control of Walking Robots by Manipulating the Zero Moment Point," *Journal of the Robotics Society of Japan*, Vol.18, No.3, pp. 359-365, 2000.
- [6] Drank Plestan, Jessy W. Grizzle, Eric R. Westervelt and Gabriel Abba: "Stable Walking of A 7-DOF Biped Robot," *IEEE Transactions on Robotics & Automation*, Vol.19, No.4, pp. 653-668, August, 2003.
- [7] Shuuji Kajita, Kazuo Tani: "Study of dynamic walk control of a biped robot on rugged terrain. Derivation and application of the linear inverted pendulum mode," *The Society of Instrument & Control Engineers*, Vol.27, No.2, pp. 177-184, 1991.
- [8] Shuuji Kajita, Kazuo Tani: "Dynamic Biped Walking Control on Rugged Terrain Using the Linear Inverted Pendulum Mode," *The Society of Instrument & Control Engineers*, Vol.31, No.10, pp. 1705-1714, 1995.
- [9] M.H.Raibert: "Legged Robots That Balance," *The MIT Press*, 1986.
- [10] Eiji Nakano, Hiroki Okubo and Hiroshi Kimura: "The Landing

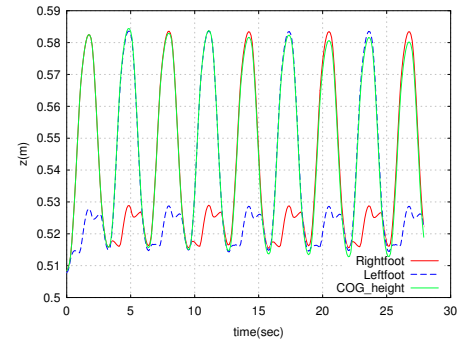


Fig. 11. Relationship between COG height and leg length in z direction

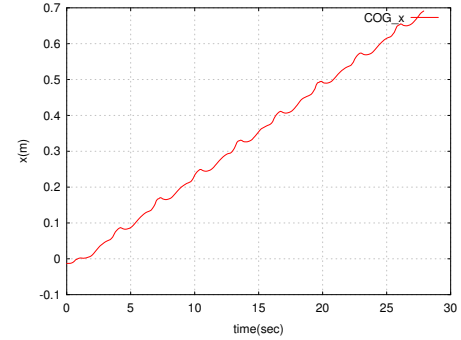


Fig. 12. COG trajectory in x axis in Σ_g

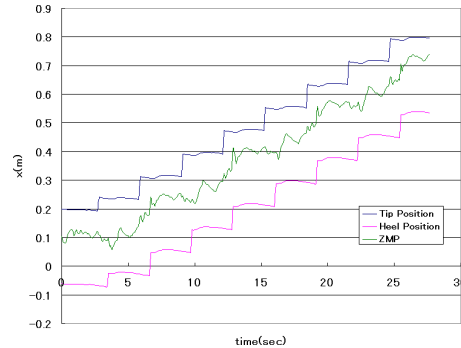


Fig. 13. ZMP in Σ_g

- Control of a Jumping Machine," *Journal of the Robotics Society of Japan*, Vol.9, No.2, pp. 169-176, 1991.
- [11] Takayuki Ikeda, Takayuki Shinohara and Tsutomu Mita: "Running Control for 3D Leg Robot Using Variable Constraint Control," *Journal of the Robotics Society of Japan*, Vol.21, No.1, pp. 94-102, 2003.
- [12] Takashi Nagasaki, Shuuji Kajita, Kazuhito Yokoi, Kenji Kaneko, Hirohisa Hirukawa and Kazuo Tanie: "Running Pattern Generation for a Humanoid Robot," *Journal of the Robotics Society of Japan*, Vol.21, No.8, pp. 902-908, 2003.
- [13] Kouhei Ohnishi: "Robust Motion Control by Disturbance Observer," *Journal of the Robotics Society of Japan*, Vol.11, No.4, pp. 486-493, 1997.
- [14] Kazuya Yoshida: "The SpaceDyn: A MATLAB Toolbox for Space and Mobile Robots," *Journal of the Society of Instrument & Control Engineers*, Vol.38, No.2, pp. 138-143, 1999.